Probing Aerogels by Multiple Quantum Filtered ^{131}Xe NMR Spectroscopy

Thomas Meersmann,*,†,‡ Michaël Deschamps,§ and Geoffrey Bodenhausen*,§

Contribution from the Department of Chemistry, Colorado State University, Fort Collins, Colorado 80523, and Département de Chimie, associé au CNRS, Ecole Normale Supérieure, 24, rue Lhomond, 75231 Paris Cedex 05, France

Received July 25, 2000. Revised Manuscript Received November 15, 2000

Abstract: At the interface between solid surfaces and cavities filled with gaseous or liquid xenon, the nuclear magnetization of ^{131}Xe ($S = {}^3/_2$) is subject to quadrupolar interactions which may lead to higher rank single-quantum coherences that can be described by tensor elements $T_{2,\pm1}$ and $T_{3,\pm1}$. This can be demonstrated by multiple-quantum filtered (MQF) NMR experiments. In gaseous xenon on Pyrex surfaces, the primary source of such coherences was shown to be coherent evolution induced by a nonvanishing average quadrupolar coupling. In this contribution, MQF NMR is applied to aerogels filled with liquid xenon to demonstrate the potential of this technique for material sciences. Xenon in the liquid phase provides a sufficient spin density to obtain reasonable signal-to-noise ratios. Coherent evolution and relaxation both contribute to the creation of higher rank coherences depending on the presence or absence of water molecules on the surface. These two processes can be distinguished experimentally and provide complementary information about the surface of the host material.

Introduction

A xenon-131 nucleus experiences an electric field gradient (EFG) if the atom is physisorbed on the surface of a host material.[1,2] The coupling between the quadrupole moment of a xenon-131 nucleus ($S = {}^3/_2$) and the EFG leads to quadrupolar splittings which may be as large as 6 MHz on Duran glass surfaces.[3] Different surface sites feature different quadrupolar couplings, either because of a variation in the strength of the xenon adsorption or because of the angle of the unique axis of the EFG tensor, believed to be parallel to the surface normal, with respect to the magnetic field. The overall quadrupolar interaction at the surface can be described as:

$$\hat{H}_Q^S(t) = \hat{H}_Q^{S(0)} + \hat{H}_Q^{S(1)}(t) \tag{1}$$

The first term $\hat{H}_Q^{S(0)}$ represents the surface-averaged and time-averaged quadrupolar interaction:[4−6]

$$\hat{H}_Q^{S(0)} = \left\langle \int_{S_{\tau_{\mathrm{NMR}}}} \frac{\mathrm{d}S'}{S_{\tau_{\mathrm{NMR}}}} \int_\tau \frac{\mathrm{d}t}{\tau} \hat{H}_Q^S(t) \right\rangle \tag{2}$$

where the integration over τ averages the quadrupolar interaction during the residence time τ of the xenon atom on a microscopic surface site dS'. The integral over the surface area accounts for the averaging of the interactions arising for a xenon atom readsorbing on different surface sites dS'. Only readsorption within a partial surface area $S_{\tau_{\mathrm{NMR}}}$ of the overall surface S need to be considered because of the intrinsic time limitation τ_{NMR} given by the relevant NMR time scale. Finally, the brackets represent the ensemble average over all xenon atoms. The resulting time-independent Hamiltonian $\hat{H}_Q^{S(0)}$ originating from the surface interactions leads to an average coherent quadrupolar evolution.

In contrast, the time-dependent part of the Hamiltonian $\hat{H}_Q^{S(1)}(t)$ represents fluctuations caused by exchange between different sites of the surface and by diffusion along the surface if the sticking time τ_s is long enough for any site hopping to occur. It is a random variable with zero average which will give rise to relaxation but not to any coherent evolution. The average coupling at the surface is scaled by the factor $\tau_s/(\tau_s + \tau_v)$ due to exchange of surface-adsorbed xenon with the bulk fluid phase, where τ_s is the mean sticking time on the surface and τ_v is the time between encounters with the surface which lead to an adsorption of a given xenon atom. The scaling reduces the effective surface coupling many orders of magnitude depending on the ratio of the surface to the bulk fluid phase volume. Previous experiments by Mehring et al.[3,6] showed that although the quadrupolar interaction on a surface is on the order of several MHz, the observed effective splitting in the gas phase is reduced to some 100 mHz for low-pressure gaseous xenon contained in a macroscopic cylindrical glass container. The average Hamiltonian describing the coherent evolution of the xenon spins can be obtained by considering the surface interaction as a first-order perturbation to the fluid-phase Zeeman Hamiltonian. This treatment is sufficient even at a low magnetic field strength of 300 nT where the xenon-131 Larmor frequency around 1 Hz is substantially larger than the effective splitting.

* Address correspondence to this author.
† Colorado State University.
‡ Current address: Materials Sciences Division, Lawrence Berkeley National Laboratory, and Department of Chemistry, University of California at Berkeley, Berkeley, CA 94720.
§ Ecole Normale Supérieure.

(1) Meersmann, T.; Smith, S. A.; Bodenhausen, G. *Phys. Rev. Lett.* **1998**, *80*, 1398−1401.
(2) Deschamps, M.; Burghardt, I.; Derouet, C.; Bodenhausen, G.; Belkic, D. *J. Chem. Phys.* **2000**, *113*, 1630−1640.
(3) Butscher, R.; Wäckerle, G.; Mehring, M. *Chem. Phys. Lett.* **1996**, *249*, 444−450.
(4) Wu, Z.; Happer, W.; Daniels, J. M. *Phys. Rev. Lett.* **1987**, *59*, 1480−1483.
(5) Raftery, D.; Long, H.; Shykind, D.; Grandinetti, P. J.; Pines, A. *Phys. Rev. A* **1994**, *50*, 567.
(6) Butscher, R.; Wäckerle, G.; Mehring, M. *J. Chem. Phys.* **1994**, *100*, 6923−6933.

10.1021/ja002747v CCC: $20.00
Published on Web 01/13/2001

Thus, the density operator of the spin system evolves under the influence of an effective Liouvillian as described by Deschamps et al.[2] where the average splitting ω_Q corresponds to the effect of $\hat{H}_Q^{S(0)}$ and the combined influences of relaxation and inhomogeneous quadrupolar broadening that cannot be refocused by a π-pulse are described by effective line widths.

Theory and Pulse Methods

The product operator formalism,[7] which is widely accepted for the description of spin-$^1/_2$ nuclei, is rather cumbersome when applied to systems containing spins with $I > {}^1/_2$. It is more convenient to represent the evolution of a quadrupolar spin system in terms of irreducible tensor operators.[8−10] In this formalism, the populations of a spin-$^3/_2$ system in thermal equilibrium at high field are described by a tensor $T_{1,0}$ of first rank and zeroth order ("Zeeman order"). This can be transformed into coherence of first rank and first-order $T_{1,\pm1}$ ("single-quantum coherence") by a 90° radio frequency (rf) pulse. Only the order of the coherence can be changed by the rf pulse, while the rank of a coherence can be altered through evolution under the combined effects of both quadrupolar interaction and relaxation. Thus $T_{1,\pm1}$ coherence may be transformed into second and third rank terms $T_{2,\pm1}$ and $T_{3,\pm1}$ ("antiphase single-quantum coherences"). Only a coherence $T_{1,\pm1}$ of first rank and first order can be directly observed in an NMR experiment. The effective quadrupolar coupling caused by interactions with the surface causes modulations of the $T_{1,\pm1}$ coherence in time domain that lead to a triplet in frequency domain.[6] Unfortunately, the line widths are usually broadened by field inhomogeneity and susceptibility effects to the extent that small splittings due to exchange between the surface and the bulk phase cannot be observed.

Alternatively, MQF NMR spectroscopy combined with a 180° pulse to refocus the effects of magnetic inhomogeneities can be employed to detect higher rank tensor elements ($T_{2,\pm1}$ and $T_{3,\pm1}$) and to obtain information about surface interactions. If the average quadrupolar coupling vanishes, no $T_{2,\pm1}$ term is generated, but $T_{3,\pm1}$ may be observed in the presence of quadrupolar relaxation. Although these terms do not directly lead to any observable signal, they can be converted back into observable coherence $T_{1,\pm1}$ under quadrupolar evolution or relaxation and they can thus be monitored indirectly. This is demonstrated in Figure 1 where four pulse sequences using multiple quantum filters are shown. The simplest double-quantum filtered (DQF) sequence in Figure 1a, which uses two 90° pulses to excite and reconvert double-quantum coherences, in effect monitors a superposition of $T_{2,\pm1}$ and $T_{3,\pm1}$ which are created during the period $2\tau_e$. The magic-angle DQF sequence (MA-DQF) shown in Figure 1b uses two magic-angle pulses with $\beta = 54.7°$ and allows one to extract solely the $T_{2,\pm1}$ term. The triple-quantum-filtered (TQF) sequence shown in Figure 1c allows one to monitor the evolution of the $T_{3,\pm1}$ term. The spectra were obtained from xenon gas contained in a plain 8 mm (o.d.) Pyrex tube at $T = 298$ K and $P = 1.2$ MPa. The spectra were taken under conditions where line broadening would not allow any splitting to be observed in a conventional single-quantum spectrum. They are closely analogous to previous experiments involving ^{23}Na cations ($S = {}^3/_2$) interacting

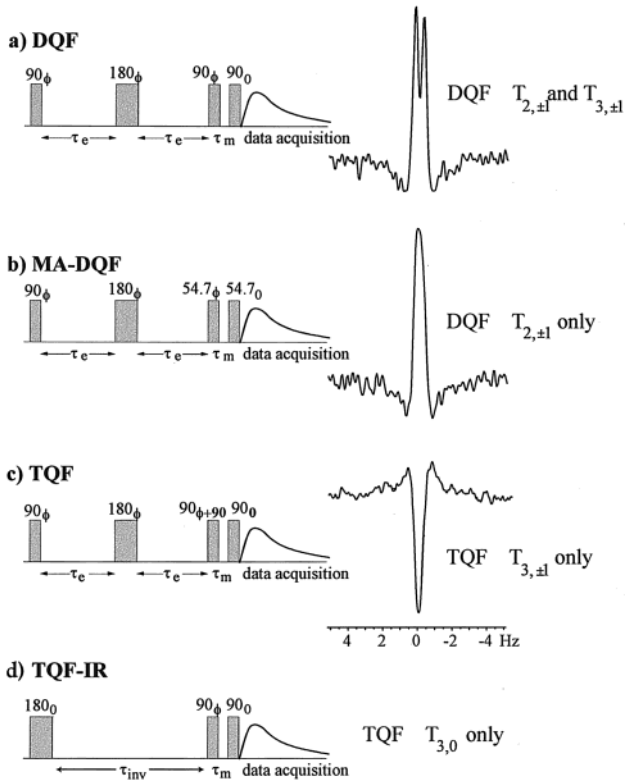

Figure 1. Pulse sequences and resulting ^{131}Xe spectra obtained in a 6 mm i.d. Pyrex tube at 7.4 T, 1.2 MPa, and 298 K: (a) double-quantum filtered pulse sequence, (b) magic-angle double-quantum filter which is a $T_{2,\pm1}$ pulse sequence, (c) triple-quantum filtered sequence, and (d) triple-quantum filtered inversion recovery pulse sequence.

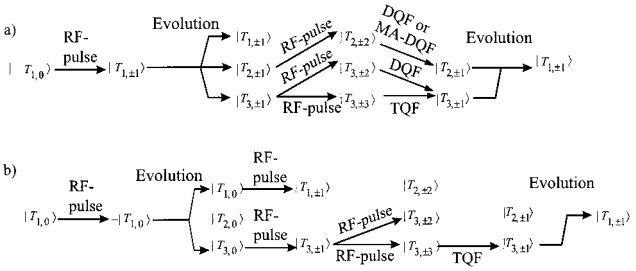

Figure 2. Schemes showing the evolution of the density operator under the influence of a coherent quadrupolar coupling and quadrupolar relaxation during the different pulse sequences: (a) evolution of the density operator observed during the DQF, MA-DQF, or TQF sequences in the presence of an average coupling and transverse relaxation and (b) evolution of the density operator during the TQF−IR sequence in the presence of multiexponential longitudinal relaxation.

with a partly oriented cartilage[11,12] and other experiments involving ^{7}Li[8] and ^{25}Mg.[13] The evolution of the density operator of the spin system for these experiments is represented in Figure 2a.

The three experiments of Figure 1a−c allow one to probe the behavior of the spin system under the combined influence of transverse relaxation and coherent quadrupolar evolution. Longitudinal relaxation may be studied by an MQF inversion recovery sequence (TQF-IR) shown in Figure 1d and explained in Figure 2b. The spin systems will only experience mono-exponential relaxation if the extreme narrowing condition is fulfilled, i.e., if $\omega_0\tau_c \ll 1$. However, longitudinal relaxation

(7) Sørensen, O. W.; Eich, G. W.; Levitt, M. H.; Bodenhausen, G.; Ernst, R. R. *Prog. NMR Spectrosc.* **1983**, *16*, 163−192.
(8) Jaccard, G.; Wimperis, S.; Bodenhausen, G. *J. Chem. Phys.* **1986**, *85*, 6282−6293.
(9) Müller, N. *Chem. Phys. Lett.* **1986**, *131*, 218−223.
(10) Müller, N.; Bodenhausen, G.; Ernst, R. R. *J. Magn. Reson.* **1987**, *75*, 297−334.
(11) Eliav, U.; Shinar, H.; Navon, G. *J. Magn. Reson.* **1992**, *98*, 223−229.
(12) Eliav, U.; Navon, G. *J. Magn. Reson. Ser. B* **1994**, *103*, 19−29.
(13) Wimperis, S. *J. Magn. Reson.* **1990**, *87*, 174−182.

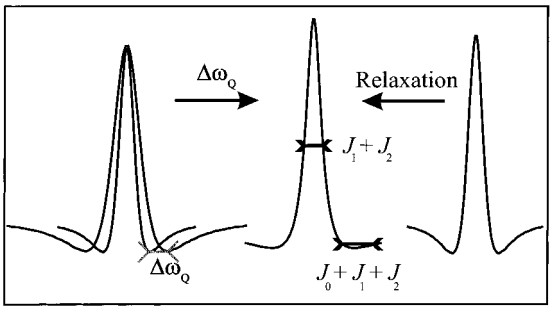

Figure 3. Roles of inhomogeneity and relaxation in line broadening. An inhomogeneous distribution of the average quadrupolar splitting is represented by $\Delta\omega_Q$. The effective relaxation rate of the two external transitions is given by $J_0 + J_1 + J_2$, and the relaxation rate of the central transition by $J_1 + J_2$.

becomes multiexponential if the motion is slowed to $\omega_0\tau_c \approx 1$. The first 180° pulse inverts the initial equilibrium state $T_{1,0}$ into $-T_{1,0}$, which is partly transformed into $T_{3,0}$ if the relaxation is multiexponential. The TQF allows one to selectively monitor the $T_{3,\pm1}$ term.[8,9] Thus, the presence of a signal in such an experiment indicates a violation of the extreme narrowing condition. This may be a powerful probe for the motions in exchanging systems.

A naïve interpretation of the behavior of the xenon-131 signals in aerogels in terms of an average Liouvillian leading to an average splitting and effective line widths may be misleading. The spectra we obtained correspond to average powder spectra as explained in Figure 3. For an isolated ^{131}Xe atom, the evolution during the period $2\tau_e$ may be described by an average Liouvillian as explained in ref 2. However, one has to take an average over different surfaces visited by different atoms during the same period. This leads to a line broadening due to the different values of the average splitting ω_Q experienced by each xenon atom. This subsequent inhomogeneous line broadening has to be taken into account in the interpretation of the decay rates we obtained from the time evolution of the density operator. Thus we only obtain effective spectral densities from a study of the combined effects of transverse quadrupolar relaxation and average quadrupolar coupling. In the following, the measured spectral densities $J(0)$, $J(\omega_0)$, and $J(2\omega_0)$ may be noted respectively as $J^{long}_{0,1,2}$(dry/wet) or $J^{trans}_{0,1,2}$(dry/wet) depending on the sequence type (probing longitudinal or transverse relaxation) and on the nature of the sample (dry stands for strongly degassed, or wet corresponds to partly degassed).

Experimental Section

Aerogels have been chosen to explore the applicability of MQF NMR of liquid xenon-131 for the study of mesoporous materials. These experiments can in principle be performed in the gas phase at moderate pressures around 1 MPa. However, to reduce the experimental time, the signals of liquid xenon have been observed with a high-pressure single-crystal sapphire tube described elsewhere.[14−16] The tubes have been filled with aerogel fragments of a few millimeter diameter and were pressurized with xenon to about 6.9 MPa at 298 K to create supercritical conditions. The actual experiments have been performed at 285 K where the xenon is in the liquid phase so that the spin density is greatly increased compared to the gas phase. Before the measurements, the aerogel samples were prepared by two different procedures to remove surface adsorbates. In one preparation, the sapphire tube with the aerogel fragments was placed in a vacuum at room temperature for about 15 min, resulting in a partial removal of the adsorbates (i.e., mainly paramagnetic oxygen, nitrogen, and water) from the surface. Since adsorbed water is only partly removed under these mild conditions, we shall refer to "wet" samples in this case. Figure 4a shows the results from ^{131}Xe MQF experiments with "wet" alumino silica aerogels of density $d = 0.1$ g/cm^3. A more vigorous removal of the surface adsorbates has been accomplished by heating an otherwise identical aerogel sample under vacuum to 350 °C for about 30 min until a pressure of 3−4 Pa was reached. Samples prepared in this manner will be referred to as "dry" samples. The results from "dry" alumino silica aerogels are shown in Figure 4b. The peak heights were compared to the intensity of the signal obtained after a single 90° pulse for normalization and the curves were fitted with the functions provided in ref 2.

Results and Discussion

The effects of Figure 4 must be due to differences in the surface structure and behavior of the wet and dry aerogels. Similar aerogels absorb water directly from moist air, leading to mass increases of up to 20%. This process is reversible and heating to temperatures above 400 K will completely dry the material. The reversibility of this process can be confirmed by MQF NMR experiments since dry aerogels exposed to water vapor revert to the behavior of wet aerogels. The removal of water leads to surfaces covered with hydroxyl groups that have stronger interactions with xenon, as evidenced by the TQF-IR signals which indicate longer sticking times of the xenon atoms. This leads to an increase in longitudinal and transverse relaxation. This effect has previously been used, but without MQF, as a means of enhancing surface contrast in MRI.[16] Furthermore, slow motion implies that $J(0) \gg J(\omega_0) > J(2\omega_0)$, leading to faster relaxation rates for the external transitions of spin $^3/_2$ and explaining why MA-DQF signals vanish in the degassed sample.

To explain the presence of coherent interactions for xenon-131 in aerogels, one has to carefully study the microscopic structure of aerogels. The aerogels comprise primary particles of 1−5 nm diameter that are interlinked together to form a mesoporous framework. This framework is fractal until a radius of about 50 nm, but it may be described as a network of pores with a 2−50 nm diameter, which is usually considered to be within the mesoscopic scale. If the xenon atoms were able to visit the whole network of cavities, one would expect a vanishing average quadrupolar coupling. However, we must invoke two arguments: First, the xenon atoms cannot easily move about locally because of slow diffusion in the liquid phase. Hence, they only experience the average coupling induced by the generally nonspherical cavity in which they are effectively confined during the measurements. Such a behavior would give an average powder spectrum, thus leading to a nonvanishing apparent splitting, as shown in Figure 3. Second, optical polarization microscopy indicates some directional heterogeneity within the aerogel fragments which may have been imposed by stress on the material during production. This suggests that the cavities in each aerogel fragment are not randomly oriented but possess a macroscopic directional preference. The consequence is that an averaged powder spectrum is observed.

The results of the fits of the curves of Figure 4 are reported in Table 1. The TQF-IR data, observed in the dry sample and fitted according to ref 8, indicate a strong violation of the extreme narrowing condition in the dry sample, due to stronger surface interactions and longer sticking times. Note that this experiment is independent from inhomogeneity effects. The spectral densities J^{long}_1(dry) and J^{long}_2(dry) obtained from TQF-

(14) Roe, D. C. *J. Magn. Reson.* **1985**, *63*, 388−391.
(15) Cusanelli, A.; Frey, U.; Richens, D. T.; Merbach, A. E. *J. Am. Chem. Soc.* **1996**, *118*, 5265−5271.
(16) Pavlovskaya, G.; Blue, A. K.; Gibbs, S. J.; Haake, M.; Cros, F.; Malier, L.; Meersmann, T. *J. Magn. Reson.* **1999**, *137*, 258−264.

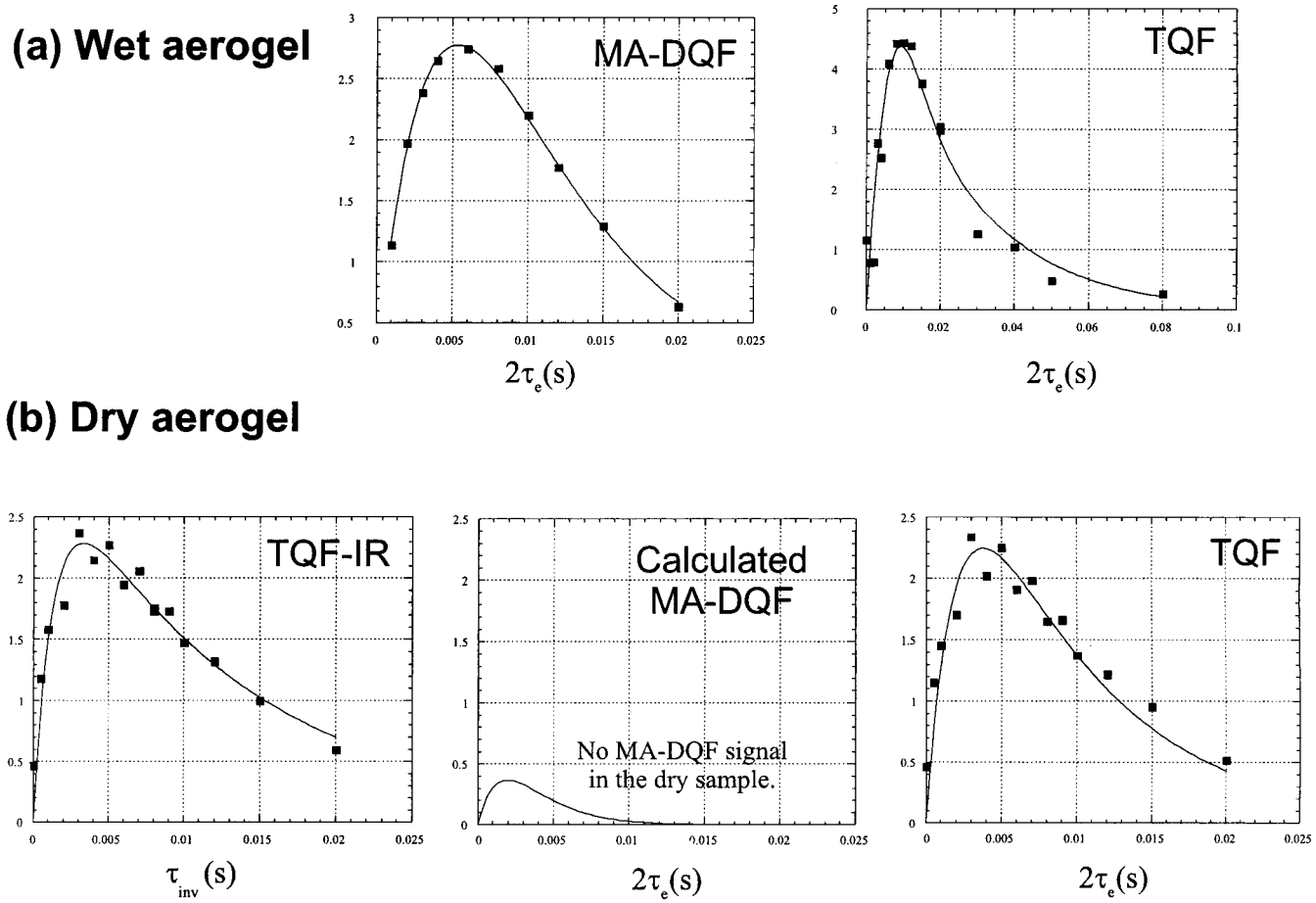

Figure 4. Experimental liquid xenon-131 signal intensities and fits for the wet (or partly degassed) and dry (or strongly degassed) aerogels of density $d = 0.1$ g/cm^3: (a) with the wet or partly degassed aerogel, no TQF−IR signals were observed, and the fits were obtained according to ref 2, and (b) in the dry or strongly degassed aerogel, only TQF and TQF-IR signals were observed and fitted, thus indicating a violation of the extreme narrowing condition. The MA-DQF signals were not observable. A theoretical MA-DQF curve has been calculated for similar conditions.

Table 1. Rates Extracted by Fitting the Curves Presented in Figure 4[a]

experiment	rate	wet	dry
TQF−IR	J_1^{long}	N/A	387 ± 71 s^{-1}
	J_2^{long}	N/A	39 ± 7 s^{-1}
MA-DQF + TQF	ω_{eff}	183 ± 66 s^{-1}	0 ± 112 s^{-1}
	J_0^{trans}	147 ± 17 s^{-1}	383 ± 7 s^{-1}
	$J_1^{trans} + J_2^{trans}$	42 ± 11 s^{-1}	$118 + 1$ s^{-1}

[a] The first two lines correspond to the spectral densities obtained from the TQF-IR experiment, and the following lines have been extracted from the combined MA-DQF and TQF experiments.

IR data cannot be interpreted in terms of a single Lorentzian $J(n\omega_0) = \tau_c/[1 + (n\omega_0\tau_c)^2]$. This tends to indicate that the underlying motions are complicated. For the wet aerogel, no TQF-IR signal could be observed, i.e., no violation of the extreme narrowing condition is apparent, indicating that the ^{131}Xe sticking time is very short in this case.

The interpretation of the MA-DQF and TQF experiments leads to distinct values for ω_{eff}, J_0^{trans}, and $J_1^{trans} + J_2^{trans}$ for the wet and dry aerogels (Table 1). These last two are different from the ones stemming from the TQF-IR experiment in the dry aerogel. As this observation is beyond the scope of this article, we chose to treat the experiments separately to draw some conclusions concerning the aerogel structure and the xenon atoms dynamics. In both dry and wet samples, we are in a regime where the coherent quadrupolar interaction is dominant. In both cases, a nonvanishing quadrupolar interaction is present, with splittings lying between 117 and 249 s^{-1} in the wet sample and between 0 and 112 s^{-1} in the dry sample. The error in the determination of the splitting in the dry sample is larger because this estimate stems from the sole TQF experiment, while the wet sample exhibits MA-DQF and TQF signals. The functions appropriate for the regime where relaxation is dominant[2] did not allow a good fit of the observed curves. Note that the splittings in the dry sample might be lower than those in the wet sample, even if the sticking time is believed to be larger. Two effects can be invoked: On the one hand, a lower splitting could be due to a modification of the structure induced by the removal of water atoms from the cavities, thus allowing xenon atoms to visit more adsorption sites and to experience a greater variety of quadrupolar couplings, which leads to a better averaging of the interaction. On the other hand, the splitting we measured is the effective splitting[2] $\omega_{eff} = (\omega_Q^2 - J_2^{trans^2})^{1/2}$. If J_2^{trans}(dry) > J_2^{long}(dry), one could explain why ω_{eff}(dry) is lower than ω_{eff}(wet) even if the average splitting ω_Q(dry) $\approx$ ω_Q(wet) remains unchanged.

Concerning the effective spectral densities extracted from the MA-DQF and TQF experiments (last two lines in Table 1), one can observe that they appear to be considerably higher in the dry sample. As shown in Figure 3, inhomogeneities may broaden the lines and lead to an overestimation of the relaxation rates. Inhomogeneities should be less important in the wet sample: water adsorbed on the surface could have a smoothing effect, masking the chemical heterogeneity of the adsorption sites. Moreover, removing water allows xenon to explore smaller

cavities previously filled with H_2O molecules, thus leading to wider spread of possible values of ω_Q. Second, if surface interactions are stronger in the dry aerogel, longer sticking times τ_S lead to stronger relaxation. These arguments explain why decay rates are larger in the dry sample compared to the wet sample.

Furthermore, in the dry sample, no MA-DQF signal could be detected. The combination of inhomogeneities and slow motion—revealed by TQF-IR signals—explains why the value of $J_0^{trans}(dry) = 383 \pm 7\ s^{-1}$ is higher than the sum of the two other spectral densities $J_1^{trans}(dry) + J_2^{trans}(dry) = 118 \pm 1\ s^{-1}$. Assuming $\omega_{eff} = 100\ s^{-1}$ in the dry aerogel, and with the values of the spectral densities above, we plotted the theoretical curve stemming from the MA-DQF experiment in Figure 4b. This signal is experimentally undetectable. The decay rate of the MA-DQF signal, which corresponds to the outer transitions, is proportional to $J_0^{trans}(dry) + J_1^{trans}(dry) + J_2^{trans}(dry)$, which is much faster than the decay rate of the TQF signal, which corresponds to the central transition, proportional to $J_1^{trans}(dry) + J_2^{trans}(dry)$.

Conclusion

The interpretation of ^{131}Xe MQF NMR would benefit from further experiments with materials that show a better macroscopic homogeneity. There is a surprisingly close analogy between the behavior of xenon-131 interacting with the surface of mesoporous materials and that of alkali-metal cations bound to slowly tumbling biological macromolecules.[11,12,17,19] A careful analysis of the combined effects of average quadrupolar couplings, quadrupolar relaxation, and inhomogeneities may provide important information concerning the surface of the aerogel and the affinity of xenon for this surface. Inhomogeneities remain the main factor limiting the interpretation of the results. The dependence of ^{131}Xe MQF spectra on the surface state may be of particular interest in combination with magnetic resonance imaging. Similar effects have been used previously to distinguish between ions in intra- and extra-cellular compartments.[19−21] Moreover, ^{131}Xe MQF NMR can be applied to opaque media in contrast to ^{131}Xe quadrupolar nutation experiments enhanced by optical pumping, and can therefore be employed to study surfaces of porous materials. Sufficient signal intensities can be achieved by liquid xenon experiments.

In conclusion, ^{131}Xe MQF NMR may be a powerful method to characterize the surface state of low-density aerogels. Due to the extreme sensitivity of the system with respect to the state of the surface, it may be possible to probe for various materials that are adsorbed on the surface. If the mesoporous material is used as a catalyst, it would be useful to know whether a chemical species remains adsorbed on the surface, i.e., to obtain knowledge about the lifetime and its relation to the catalytic efficiency of such materials. One could calibrate the effect of these phenomena, such as remaining species adsorbed on the surface, on xenon-131 spin dynamics to obtain a powerful probe of the microscopic state of the surface.

Acknowledgment. We would like to thank Dr. Jean-Pierre Korb, who provided us with aerogels samples, and Mr. Roger Ith, for the manufacturing of the sapphire tube assembly. We gratefully acknowledge Dr. Timothy Cross, Dr. Alan Marshall, and Dr. Jack Crow of the National High Magnetic Field Laboratory in Tallahassee, FL supported by the National Science Foundation Cooperative Agreement DMR-9527035 and the State of Florida.

JA002747V

(17) Chung, C.-W.; Wimperis, S. *J. Magn. Reson.* **1990**, *88*, 440−447.
(18) Meersmann, T.; Haake, M. *Phys. Rev. Lett.* **1998**, *81*, 1211−1214.
(19) *Relaxation Mechanisms of Intra- and Extracellular Sodium*; Seo, Y., Murakami, M., Ichikawa, O., Eds.: National Institute for Physiological Sciences, Okazaki, Japan, November 13−16, 1991.
(20) Griffey, R. H.; Griffey, B. V.; Matwiyoff, N. A. *Magn. Reson. Med.* **1990**, *13*, 305.
(21) Kemp-Harper, R.; Styles, P.; Wimperis, S. *J. Magn. Reson. Ser B* **1995**, *108*, 280−284.